International Atomic Energy Agency

INDC(CCP)-327/L

INDC INTERNATIONAL NUCLEAR DATA COMMITTEE

TRANSLATION OF SELECTED PAPERS

PUBLISHED IN YADERNYE KONSTANTY (NUCLEAR CONSTANTS 4, 1989)

(Original Report in Russian was distributed
as INDC(CCP)-311/G)

Translated by A. Lorenz
for the
International Atomic Energy Agency

March 1991

IAEA NUCLEAR DATA SECTION, WAGRAMERSTRASSE 5, A-1400 VIENNA

INDC(CCP)-327/L

TRANSLATION OF SELECTED PAPERS

PUBLISHED IN YADERNYE KONSTANTY (NUCLEAR CONSTANTS 4, 1989)

(Original Report in Russian was distributed
as INDC(CCP)-311/G)

Translated by A. Lorenz
for the
International Atomic Energy Agency

March 1991

Reproduced by the IAEA in Austria
April 1991

91-01295

Contents

NEUTRON DATA FOR THERMAL REACTOR CALCULATIONS

L.P. Abagyan, M.P. Prosvetova, M.S. Yudkevich

Abstract

This paper gives a description of the evaluated neutron data library KORT-88 for neutron energies below 5 eV. This library consists of neutron cross-sections and resonance integrals for nuclides with Z < 90.

The KORT library of evaluated neutron data whas been described previously in references [1] and [2]. This data library includes cross-sections for energies below 5 eV and is designed for the calculation of thermal neutron spectra in nuclear reactors as well as additional information for a variety of applications. Since a considerable amount of new experimental information and other nuclear data evaluations have been published since the publication of the original KORT library, it was deemed timely to perform a re-evluation of these data, and at the same time to broaden the composition of the library. This work is now finished, and the new KORT-88 library is completed. It now includes data for all naturally stable isotopes with Z < 90 and their naturally occurring mixtures - altogether 343 materials. The data library is recorded on computer media.

The following information is included for each istope:

- A - the atomic mass,
- ε - natural abundance,
- QA - energy release upon neutron absorption,
- SIG - thermal scattering, absorption, and (n,γ), (n,p) and (n,α) cross-sections (E=0.0253 eV),
- RI(E_c) - resonance integrals for capture and other reactions (E_c > 0.5 eV),
- σ(E) - neutron energy dependence of the cross-section,
- G - Westcott g-factor.

Existing uncertainties or ambiguities in the knowledge of the cross-sections and resonance integrals are given in the comments. The cross-sections and resonance integrals for those (n,γ) reactions which result in an isomer are given there as well.

KORT-88 data for isotopes with Z≤37 are given in Table I; the energy dependence of the cross-section $\sigma_c(E)$ for all of these isotopes follows the "1/V" law:

$$\left[\sigma_a = const., \qquad \sigma_c(E) = \sigma_c(0.0253\ eV)\sqrt{\frac{0.0253}{E,\ eV}} \right]$$

Isotopes with Z>37 are given in Table II. The Westcott g-factor is included for those nuclides, whose cross-section $\sigma_c(E)$ does not have a "1/V" dependence, and for which there is information in the LIPAR-87 [3] resonance parameter data library.

The last version of the LIPAR-87 data library is in agreement with the KORT-88 data library.

TABLE I. THERMAL CROSS-SECTIONS AND RESONANCE INTEGRALS FOR ISOTOPES WITH Z<38 FROM THE KORT-88 DATA LIBRARY

N/N	Isotope	ε	σ_e, barn	σ_c^o, barn	RI, barn
1	1-H		20.491	0.3326	0.149
2	1-D		3.390	0.000519	0.00023
3	2-HE		0.73	0.007	0.0031
4	2-HE-3	0.0000014	1.9	5327.	2400.
5	2-HE-4	1.0000	0.73	0.0	0.0
6	3-LI		0.95	70.54	32.
7	3-LI-6	0.075	0.75	940.	423.
8	3-LI-7	0.925	0.97	0.0454	0.020
9	4-BE-9	1.00	6.151	0.008	0.0036
10	5-B		4.27	767.	345.
11	5-B -10	0.198	2.23	3837.	1727.
12	5-B -11	0.802	4.84	0.0055	0.0025
13	6-C		4.74	0.0035	0.00155
14	6-C -12	0.9889	4.746	0.00353	0.00159
15	6-C -13	0.0111	4.19	0.00137	0.0017
16	7-N		10.03	1.90	0.9
17	7-N -14	0.9963	10.05	1.905	0.85
18	7-N -15	0.0037	4.59	0.000024	0.00011
19	8-O		3.761	0.00028	0.00013
20	8-O -16	0.9976	3.761	0.00019	0.00009
21	8-O -17	0.00038	3.61	0.2355	0.106
22	8-O -18	0.00202	2.7	0.00016	0.00007
23	9-F -19	1.0000	4.04	0.0096	0.004
24	10-NE		2.415	0.039	0.0188
25	10-NE-20	0.9051	2.47	0.037	0.0175
26	10-NE-21	0.0027	5.1	2.20	0.98
27	10-NE-22	0.0922	1.705	0.0455	0.023
28	11-NA-23	1.0000	3.025	0.530	0.31
29	12-MG		3.414	0.063	0.038
30	12-MG-24	0.7899	3.74	0.051	0.032
31	12-MG-25	0.1000	1.56	0.190	0.098
32	12-MG-26	0.1101	2.83	0.0382	0.026
33	13-AL-27	1.0000	1.413	0.231	0.17
34	14-SI		2.044	0.171	0.127
35	14-SI-28	0.9223	1.992	0.177	0.110
36	14-SI-29	0.0467	2.79	0.101	0.71
37	14-SI-30	0.031	2.49	0.107	0.71
38	15-P -31	1.0000	3.134	0.172	0.085

TABLE I. (continued)

N/N	Isotope	$\mathcal{E}$	σ_e barn	σ_c^o, barn	RI, barn
39	16-S		0.979	0.53	0.24
40	16-S -32	0.9503	0.9432	0.537	0.24
41	16-S -33	0.0075	2.8	0.542	0.24
42	16-S -34	0.0421	1.6	0.227	0.10
43	16-S -36	0.0001	1.50	0.20	0.17
44	17-CL		15.8	33.5	15.
45	17-CL-35	0.7577	20.6	44.09	19.8
46	17-CL-37	0.2423	1.15	0.433	0.30
47	18-AR		0.647	0.675	0.43
48	18-AR-36	0.00337	73.7	5.2	2.5
49	18-AR-38	0.00063	1.5	0.8	0.4
50	18-AR-40	0.996	0.41	0.66	0.41
51	19-K		2.04	2.1	1.1
52	19-K -39	0.93258	2.00	2.1	1.1
53	19-K -40	0.00012	2.04	34.79	15.
54	19-K -41	0.0673	2.5	1.46	1.42
55	20-CA		2.9	0.43	0.23
56	20-CA-40	0.96937	3.01	0.4125	0.22
57	20-CA-42	0.00647	1.2	0.680	0.39
58	20-CA-43	0.00135	2.93	6.2	3.93
59	20-CA-44	0.0209	0.41	0.88	0.56
60	20-CA-46	0.00004	0.79	0.74	0.32
61	20-CA-48	0.00187	0.25	1.09	0.89
62	21-SC-45	1.0000	22.4	27.2	12.0
63	22-TI		4.10	6.10	3.1
64	22-TI-46	0.082	2.78	0.59	0.30
65	22-TI-47	0.074	3.1	1.7	1.5
66	22-TI-48	0.738	4.1	7.84	3.9
67	22-TI-49	0.054	0.7	2.2	1.2
68	22-TI-50	0.052	3.7	0.179	0.12
69	23-V		4.8	5.08	2.8
70	23-V -50	0.0025	7.1	41.5	43.
71	23-V -51	0.9975	4.8	4.9	2.7
72	24-CR		3.38	3.10	1.6
73	24-CR-50	0.0435	2.41	15.9	7.8
74	24-CR-52	0.8379	2.96	0.76	0.48
75	24-CR-53	0.095	7.78	18.2	8.9
76	24-CR-54	0.0236	2.54	0.36	0.18
77	25-MN-55	1.0000	2.2	13.3	14.6
78	26-FE		11.44	2.59	1.4
79	26-FE-54	0.058	2.16	2.14	1.2
80	26-FE-56	0.9172	12.27	2.63	1.4
81	26-FE-57	0.022	2.13	2.44	1.6
82	26-FE-58	0.0028	3.19	1.27	1.4
83	27-CO-59	1.0000	6.00	37.2	74.
84	28-NI		18.0	4.47	2.2
85	28-NI-58	0.6827	25.3	4.6	2.2
86	28-NI-60	0.261	0.98	2.9	1.5
87	28-NI-61	0.0113	9.0	2.5	1.5
88	28-NI-62	0.0359	9.1	14.5	6.6
89	28-NI-64	0.0091	0.0017	1.80	1.16
90	29-CU		7.87	3.78	4.2
91	29-CU-63	0.692	5.1	4.50	4.97
92	29-CU-65	0.308	14.1	2.17	2.19
93	30-ZN		4.08	1.11	2.8
94	30-ZN-64	0.4858	3.6	0.9	1.40
95	30-ZN-66	0.279	4.4	0.7	1.77
96	30-ZN-67	0.041	3.0	6.8	25.2
97	30-ZN-68	0.188	5.4	1.070	3.1
98	30-ZN-70	0.0062	3.0	0.0917	0.86
99	31-GA		7.0	2.9	22.
100	31-GA-69	0.601	8.2	1.68	15.6
101	31-GA-71	0.399	5.2	4.71	31.
102	32-GE		8.53	2.2	6.0
103	32-GE-70	0.205	12.4	3.1	2.30
104	32-GE-72	0.274	9.0	0.93	0.76

TABLE I. (continued)

N/N	Isotope	ε	σ_e barn	σ_c°, barn	RI, barn
105	32-GE-73	0.078	4.6	14.	63.7
106	32-GE-74	0.365	6.8	0.48	1.0
107	32-GE-76	0.078	8.7	0.15	1.8
108	33-AS-75	1.0000	5.43	4.5	61.
109	34-SE		6.3	11.7	12.0
110	34-SE-74	0.0087	7.1	51.8	520.
111	34-SE-76	0.09	18.4	85.	40.
112	34-SE-77	0.076	8.43	42.	32.
113	34-SE-78	0.235	8.40	0.43	4.8
114	34-SE-80	0.498	6.95	0.61	2.0
115	34-SE-82	0.0923	5.0	0.044	0.08
116	35-BR		6.1	6.9	89.
117	35-BR-79	0.5069	6.1	11.0	127.
118	35-BR-81	0.4931	6.1	2.7	50.
119	36-KR		7.50	25.	49.
120	36-KR-78	0.0036	7.5	6.2	19.5
121	36-KR-80	0.0227	7.5	11.5	56.
122	36-KR-82	0.116	7.5	28.	190.
123	36-KR-83	0.115	7.5	180.	210.
124	36-KR-84	0.5697	7.5	0.110	3.2
125	36-KR-86	0.173	7.5	0.003	0.10
126	37-RB		6.4	0.38	6.0
127	37-RB-85	0.7217	6.2	0.48	7.5
128	37-RB-87	0.2783	6.6	0.120	2.2

TABLE II. THERMAL CROSS-SECTIONS AND RESONANCE INTEGRALS FOR ISOTOPES WITH Z>37 FROM THE KORT-88 DATA LIBRARY

N/N	Isotope	ε	σ_e, barn	σ_c°, barn	U *	G	RI, barn
1	38-SR		10.	1.28	R		10.
2	38-SR-84	0.0056	10.	0.95	V		7.4
3	38-SR-86	0.0980	10.	1.04	V		5.2
4	38-SR-87	0.0700	10.	16.	R		120.
5	38-SR-88	0.8264	10.	0.0058	V		0.065
6	39-Y -89	1.0000	7.67	1.28	V		1.0
7	40-ZR		6.1	0.19	V		0.96
8	40-ZR-90	0.5150	5.3	0.011	V		0.18
9	40-ZR-91	0.1120	10.7	1.24	V		4.9
10	40-ZR-92	0.1710	4.9	0.220	V		0.66
11	40-ZR-94	0.1740	6.1	0.048	V		0.31
12	40-ZR-96	0.0280	6.3	0.023	V		5.6
13	41-NB-93	1.0000	6.37	1.15	V		9.4
14	42-MO		5.74	2.55	V		25.
15	42-MO-92	0.1480	6.4	0.019	V		0.81
16	42-MO-94	0.0930	5.7	0.015	V		0.82
17	42-MO-95	0.1590	6.1	13.4	V		108.
18	42-MO-96	0.1670	4.8	0.5	V		24.
19	42-MO-97	0.0960	6.5	2.5	V		15.
20	42-MO-98	0.2410	5.8	0.130	V		6.9
21	42-MO-100	0.0960	5.3	0.20	V		3.75
22	44-RU		6.5	2.56	R		41.0
23	44-RU-96	0.0552	6.5	0.29	V		7.34
24	44-RU-98	0.0186	6.5	8.0	V		
25	44-RU-99	0.1270	6.5	5.0	R		195.
26	44-RU-100	0.1260	6.5	5.8	V		11.2
27	44-RU-101	0.1700	4.3	3.4	R		100.
28	44-RU-102	0.3162	6.9	1.21	V		4.2
29	44-RU-104	0.1870	8.4	0.32	V		4.3
30	45-RH-103	1.0000	5.9	146.0	R	1.023	1045.
31	46-PD		4.2	6.9	R		88.0
32	46-PD-102	0.0100	3.4	4.8	V		10.0
33	46-PD-104	0.1100	3.4	0.6	V		16.

TABLE II. (continued)

N/N	Isotope	ε	σ_e barn	σ_c°, barn	U *	G	RI, barn
34	46-PD-105	0.2220	5.0	14.7	R		98.0
35	46-PD-106	0.2730	5.1	0.305	V		5.73
36	46-PD-108	0.2670	3.4	12.2	V		230.
37	46-PD-110	0.1180	3.4	0.227	V		3.1
38	47-AG		5.08	63.2	R	1.003	760.
39	47-AG-107	0.5183	7.4	37.6	R	0.998	105.
40	47-AG-109	0.4817	2.55	91.0	R	1.005	1470.
41	48-CD		8.6	2524.	R		67.
42	48-CD-106	0.0125	5.1	0.9	V		4.
43	48-CD-108	0.0089	4.1	1.1	V		16.7
44	48-CD-110	0.1251	4.3	0.9	V		42.
45	48-CD-111	0.1281	5.	8.	R		53.
46	48-CD-112	0.2413	7.5	0.9	V		13.
47	48-CD-113	0.1222	29.3	20640.	R	1.338	390.
48	48-CD-114	0.2872	5.2	0.336	V		13.
49	48-CD-116	0.0747	6.4	0.075	V		1.35
50	49-IN		2.65	193.8	R		3170.
51	49-IN-113	0.0430	3.75	12.0	R		310.
52	49-IN-115	0.9570	2.6	202.	R	1.019	3300.
53	50-SN		4.88	0.63	R		6.4
54	50-SN-112	0.0100	4.9	1.01	V		29.
55	50-SN-114	0.0067	4.6	0.115	V		5.1
56	50-SN-115	0.0038	4.9	30.	V		29.
57	50-SN-116	0.1470	4.26	0.14	V		13.7
58	50-SN-117	0.0775	5.2	2.3	R		16.
59	50-SN-118	0.2430	4.26	0.22	V		4.7
60	50-SN-119	0.0860	4.55	2.2	R		4.2
61	50-SN-120	0.3240	5.17	0.141	V		1.25
62	50-SN-122	0.0456	4.1	0.181	V		0.81
63	50-SN-124	0.0564	4.41	0.134	V		8.032
64	51-SB		4.2	5.1	R		168.
65	51-SB-121	0.5730	4.2	5.9	R		200.
66	51-SB-123	0.4270	4.2	4.16	V		125.
67	52-TE		3.94	4.7	R		56.
68	52-TE-120	0.0009	3.3	2.34	V		
69	52-TE-122	0.0250	4.4	2.90	V		64.
70	52-TE-123	0.0089	3.94	418.0	R		5630.
71	52-TE-124	0.0460	3.8	6.8	V		5.9
72	52-TE-125	0.0701	4.0	1.55	V		21.
73	52-TE-126	0.1871	3.9	1.04	V		8.0
74	52-TE-128	0.3170	4.1	0.215	V		1.66
75	52-TE-130	0.3450	3.70	0.29	V		0.46
76	53-I -127	1.0000	3.54	6.2	V		147.
77	54-XE		3.	23.9	R		265.
78	54-XE-124	0.0010	3.	165.	R		3600.
79	54-XE-126	0.0009	3.	3.5	V		60.
80	54-XE-128	0.0191	3.	6.5	V		105.
81	54-XE-129	0.2640	3.	21.	V		250.
82	54-XE-130	0.0410	3.	6.45	V		14.9
83	54-XE-131	0.2120	25.	85.	R		900.
84	54-XE-132	0.2690	3.	0.45	V		4.6
85	54-XE-134	0.1040	3.	0.265	V		0.3
86	54-XE-136	0.0890	3.	0.26	V		0.74
87	55-CS-133	1.0000	5.8	29.	R		437.
88	56-BA		3.3	1.2	V		9.3
89	56-BA-130	0.0011	1.6	15.	V		235.
90	56-BA-132	0.0010	7.6	7.0	V		3.3
91	56-BA-134	0.0242	4.08	2.0	V		37.
92	56-BA-135	0.0659	3.30	5.8	V		110.
93	56-BA-136	0.0785	3.02	0.64	V		1.6
94	56-BA-137	0.1123	5.9	4.1	V		4.8
95	56-BA-138	0.7170	2.93	0.35	V		0.32
96	57-LA		10.13	8.97	R		12.1
97	57-LA-138	0.0009	10.15	57.2	R		409.
98	57-LA-139	0.9991	10.13	8.93	R		11.8
99	58-CE		2.85	0.63	V		3.7

TABLE II. (continued)

N/N	Isotope	ε	σ_e barn	σ_c°, barn	U	G	RI, barn
100	58-CE-136	0.0019	3.	7.25	V		58.
101	58-CE-138	0.0025	3.	1.115	V		
102	58-CE-140	0.8848	2.83	0.57	V		0.47
103	58-CE-142	0.1108	3.0	0.95	V		1.15
104	59-PR-141	1.0000	2.54	11.5	V		17.4
105	60-ND		16.	48.8	R	0.997	42.
106	60-ND-142	0.2720	7.5	18.6	R	0.999	9.0
107	60-ND-143	0.1220	82.	319.	R	0.996	130.
108	60-ND-144	0.2380	1.0	3.6	V		3.9
109	60-ND-145	0.0830	20.5	42.	R	0.9998	240.
110	60-ND-146	0.1720	9.5	1.40	V		2.7
111	60-ND-148	0.0570	4.0	2.5	V		18.
112	60-ND-150	0.0560	3.5	1.2	V		15.
113	62-SM		30.	5552.0	R	1.669	1400.
114	62-SM-144	0.0310	3.	1.6	V		2.4
115	62-SM-147	0.1510	4.	56.6	R	0.994	737.
116	62-SM-148	0.1130	4.2	2.4	V		27.
117	62-SM-149	0.1390	172.	39420.	R	1.708	3450.
118	62-SM-150	0.0740	10.3	108.	R	0.994	338.
119	62-SM-152	0.2660	5.8	202.	R	1.003	2970.
120	62-SM-154	0.2260	13.	8.3	V		35.5
121	63-EU		7.8	4564.	R	0.933	2320.
122	63-EU-151	0.4790	7.8	9200.	R	0.932	3360.
123	63-EU-153	0.5210	7.7	312.	R	0.980	1450.
124	64-GD		169.	48780.	R	0.851	400.
125	64-GD-152	0.0020	17.	732.	R	0.978	760.
126	64-GD-154	0.0210	6.0	85.0	R	0.992	335.
127	64-GD-155	0.1480	59.	60710.	R	0.844	1355.
128	64-GD-156	0.2060	5.2	1.8	V		110.
129	64-GD-157	0.1570	1005.	233500.	R	0.852	760.
130	64-GD-158	0.2480	3.6	2.2	V		73.
131	64-GD-160	0.2180	3.6	0.77	V		8.4
132	65-TB-159	1.0000	6.92	23.4	R		418.
133	66-DY		106.	940.	R		1480.
134	66-DY-156	0.0006	6.1	33.	R		884.
135	66-DY-158	0.0010	6.0	43.	R		120.
136	66-DY-160	0.0230	3.4	56.	R	1.008	1240.
137	66-DY-161	0.1901	24.	600.	R	0.990	1200.
138	66-DY-162	0.2551	0.34	199.	R	1.005	2760.
139	66-DY-163	0.2491	3.7	125.	R	1.011	1470.
140	66-DY-164	0.2811	330.	2650.	R	0.988	340.
141	67-HO-165	1.0000	8.65	64.7	R		670.
142	68-ER		8.1	158.	R	1.067	740.
143	68-ER-162	0.0014	5.3	29.	R	0.882	514.
144	68-ER-164	0.0156	8.5	2.5	R	1.002	121.
145	68-ER-166	0.3340	14.	19.4	V		109.
146	68-ER-167	0.2290	1.6	653.	R	1.071	2970.
147	68-ER-168	0.2710	8.4	2.79	V		41.
148	68-ER-170	0.1490	11.0	5.8	V		58.
149	69-TM-169	1.0000	6.3	103.	R		1710.
150	70-YB		23.4	35.	R		183.
151	70-YB-168	0.0014	23.	3470.	R		30500.
152	70-YB-170	0.0310	5.85	11.4	R		320.
153	70-YB-171	0.1441	3.4	48.6	R		340.
154	70-YB-172	0.2191	11.3	0.8	V		25.
155	70-YB-173	0.1621	3.8	17.1	R		400.
156	70-YB-174	0.3162	46.3	69.4	V		27.
157	70-YB-176	0.1261	9.66	2.85	V		6.3
158	71-LU		6.8	83.	R	1.465	622.
159	71-LU-175	0.9739	6.0	23.	R	0.997	610.
160	71-LU-176	0.0261	34.	2344.	R	1.637	1160.
161	72-HF		10.9	105.1	R	1.013	2000.
162	72-HF-174	0.0016	15.	561.	R	0.978	436.
163	72-HF-176	0.0520	5.6	23.5	R	1.003	890.
164	72-HF-177	0.1861	3.	377.	R	1.020	7240.
165	72-HF-178	0.2711	4.5	84.	R	1.003	1950.

TABLE TT. (continued)

N/N	Isotope	ε	σ_e, barn	σ_c°, barn	U *	G	RI, barn
166	72-HF-179	0.1370	7.4	41.	R	1.003	480.
167	72-HF-180	0.3522	22.0	12.9	R	0.9995	35.
168	73-TA		6.12	20.6	R		660.
169	73-TA-180	0.0001	6.1	563.0	R		1349.
170	73-TA-181	0.9999	6.12	20.5	R	1.004	660.
171	74-W		5.20	18.4	R	1.002	360.
172	74-W -180	0.0013	5.30	3.5	R	1.002	214.
173	74-W -182	0.2630	8.8	20.9	R	1.003	600.
174	74-W -183	0.1430	2.5	10.1	R	1.000	350.
175	74-W -184	0.3067	8.1	1.64	V		16.
176	74-W -186	0.2860	0.084	38.2	R	1.001	525.
177	75-RE		11.3	89.7	R		830.
178	75-RE-185	0.3740	10.6	112.	R	1.005	1717.
179	75-RE-187	0.6260	11.8	76.4	R	0.982	300.
180	76-OS		15.5	16.9	R		160.
181	76-OS-184	0.0002	15.	954.	R		600.
182	76-OS-186	0.0160	18.	80.	R		280.
183	76-OS-187	0.0160	7.5	320.	R		500.
184	76-OS-188	0.1330	7.7	4.7	V		152.
185	76-OS-189	0.1610	15.5	25.	R		674.
186	76-OS-190	0.2640	16.3	17.1	V		58.
187	76-OS-192	0.4098	17.9	2.0	V		4.6
188	77-IR		14.2	426.	R		2150.
189	77-IR-191	0.3730	15.	954.	R		3500.
190	77-IR-193	0.6270	13.	111.	R		1350.
191	78-PT		12.4	10.3	V		140.
192	78-PT-190	0.0001	12.4	152.	V		72.
193	78-PT-192	0.0079	12.3	10.	R		115.
194	78-PT-194	0.3290	14.0	1.44	V		4.
195	78-PT-195	0.3380	10.1	27.5	R		365.
196	78-PT-196	0.2530	12.3	0.72	V		5.1
197	78-PT-198	0.0720	7.7	3.7	V		54.
198	79-AU-197	1.0000	5.3	98.66	R	1.005	1560.
199	80-HG		26.5	372.	V		86.7
200	80-HG-196	0.0015	26.5	3080.	R		472.
201	80-HG-198	0.1000	18.0	2.0	V		71.
202	80-HG-199	0.1681	65.7	2150.	R		435.
203	80-HG-200	0.2311	18.0	1.4	V		2.1
204	80-HG-201	0.1321	18.0	7.8	V		30.
205	80-HG-202	0.2982	18.0	4.9	V		4.2
206	80-HG-204	0.0690	18.0	0.43	V		0.85
207	81-TL		10.0	3.43	V		12.9
208	81-TL-203	0.2950	6.3	11.4	V		43.0
209	81-TL-205	0.7050	11.6	0.104	V		0.62
210	82-PB		11.2	0.173	V		0.14
211	82-PB-204	0.0142	11.2	0.66	V		2.0
212	82-PB-206	0.2413	11.2	0.031	V		0.097
213	82-PB-207	0.2213	11.26	0.71	V		0.39
214	82-PB-208	0.5232	11.26	0.00049	V		0.0020
215	83-BI-209	1.0000	9.300	0.0338	V		0.19

U * - Type of cross-section energy dependence up to 5 eV:

V - 1/V energy dependence,
R - taking resonances into account.

REFERENCES

[1] ABAGYAN, L.P., YUDKEVICH, M.S., Problems of Atomic Science and Technology. Ser. Nuclear Constants 4 43 (1981) 24 (in Russian).

[2] ABAGYAN, L.P., YUDKEVICH, M.S., Problems of Atomic Science and Technology. Ser. Nuclear Constants 1 40 (1981) 39 (in Russian).

[3] ABAGYAN, L.P., TEBIN, V.V., YUDKEVICH, M.S., "CROSS - set of computer programs and data files for the calculation of cross-sections in the resolved resonance region", Institute of Atomic Energy Preprint IAE-4009/5, Moscow (1984) (in Russian).

EVALUATION OF ^{14}N NEUTRON DATA

A.I. Blokhin, S.A. Badikov, N.N. Buleeva, A.G. Gusseinov,
M.A. Gusseinov, V.S. Masterov, V.G. Pronyaev,
N.S. Rabotnov, N.N. Titarenko

Abstract

A short description of the ^{14}N data file is given. Experimental data on the total, (n,α) and (n,p) cross-sections, not used in the ENDF/B-IV data library, were taken into account. A new evaluation of σ_{tot} from 0.46 to 9 MeV was performed by fitting the experimental results using the Pade approximation; the σ(n,α) and σ(n,p) cross-sections were re-evaluated by modifying the evaluations given in ENDF/B-IV. Most other cross-sections were recalculated using theory.

The ^{14}N isotope is the major component of natural nitrogen (99.6%). The low threshold of charged particle yielding reactions (the threshold of the (n,p) reaction is practically zero and has a significant thermal cross-section) makes it an important source of hydrogen and helium in nitrogen-bearing fuel. Inasmuch as Morgan's [1] (n,p) and (n,α) data as well as the improved total cross-section data, originally published in reference [2], were not included in the well-documented ENDF/B-IV evaluation [3], it was decided to re-evaluate these data, and to prepare a completely new evaluated file for ^{14}N.

The data published in reference [2], which are the most detailed of all of the available total cross-section data (see references [4] to [7]), were taken as the basis for this evaluation. The authors of reference [2] corrected the original data by using a more exact sample thickness into account which increased the value of the cross-section by a few percent with respect to the values used in reference [3]. In the energy interval of 0.46 to 9.0 MeV the data [2] were averaged using the PADE2 [8] computer program based on the rational approximation model described in detail in reference [9]. In the application of this approximation method, the given energy range was subdivided into nine intervals which were analyzed individually, making sure at

the same time that the continuity of the cross-section at the junctures of the individual intervals was not interupted (see also the neutron data evaluation of ^{15}N described in reference [10]). In this rational approximation model, the position and the half-width of resonances of the total cross-section are represented as the real and imaginary parts of the complex roots of a polynomial which is the denominator of the approximating function. A comparison of the results of this analysis with published reference data [11] shows good agreement in most cases; in view of this agreement, this theoretical analysis could also serve as an additional means to check on the quality of the evaluation.

The total cross-section data published in reference [3], which were used outside of the boundaries of the chosen intervals, provided good continuity of the data at the boundary points. The comparison of the results of our evaluation of the total cross-section with the ENDF/B-IV evaluation up to 9 MeV is shown in Figs. 1a and 1b.

The evaluation of the inelastic cross-section as well as of the (n,p), (n,d), (n,t) and (n,α) reaction processes, including the excitation of discrete levels of the reaction product nuclides was performed in the framework of the Hauser-Feshbach-Moldauer model using the CMT-80 computer program [12]. The properties of the discrete levels were taken from the compilations published in references [13] and [14]. The optical model parameters used in these calculations were selected from the description of the total cross-section in the neutron energy range from 8.5 to 30 MeV given in reference [2]; the values of these commonly used optical model parameters are:

$$
\begin{array}{lll}
V = 54.0 - 0.8\,E_n & & W_D = 26.0 + 0.2\,E_n \\
V_{so} = 5.5 & r_0 = 1.209 & r_D = 1.415 \\
r_{so} = 1.15 & a_0 = 0.105 & a_{so} = 0.5
\end{array} \qquad (1)
$$

The optical model parameters for the charged particles were determined on the basis of systematics described in reference [16]. The calculation of the (n,n'), (n,p), (n,d), (n,t) and (n,α) reaction cross-sections was performed with the use of a

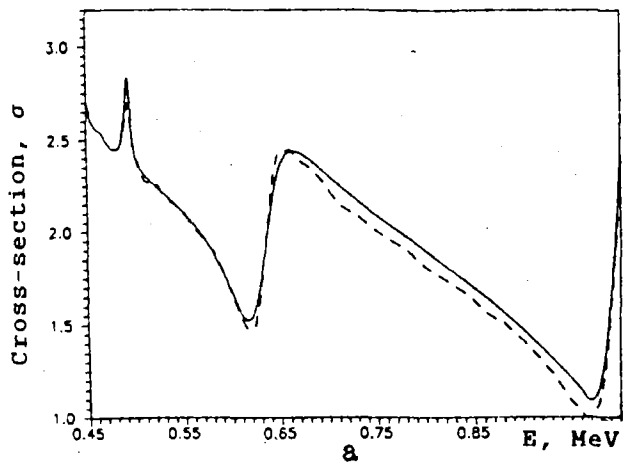

Fig. 1. Comparison of results of the evaluation of the total ^{14}N neutron cross-section performed in this work (continuous curves) with the ENDF/B-IV evaluation [3] in different energy intervals. Experimental data from reference [2], which were also used in our evaluation, are shown in Fig. 1C.

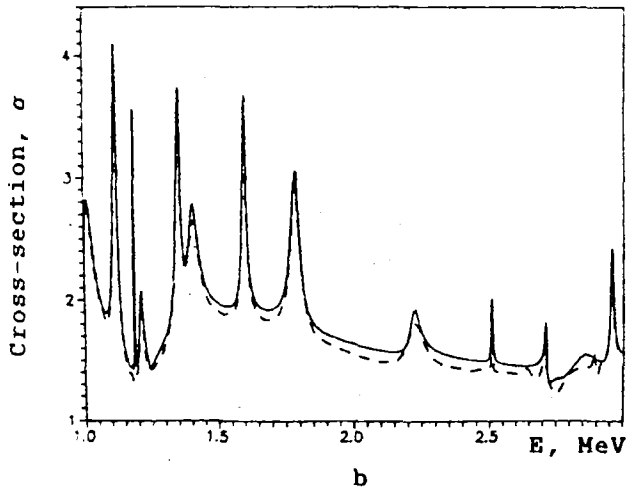

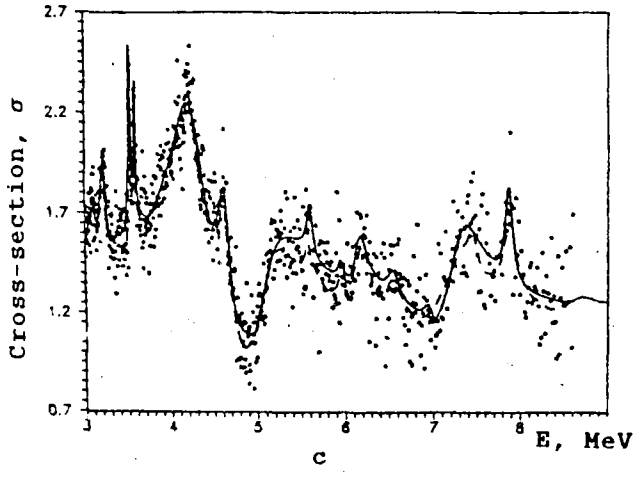

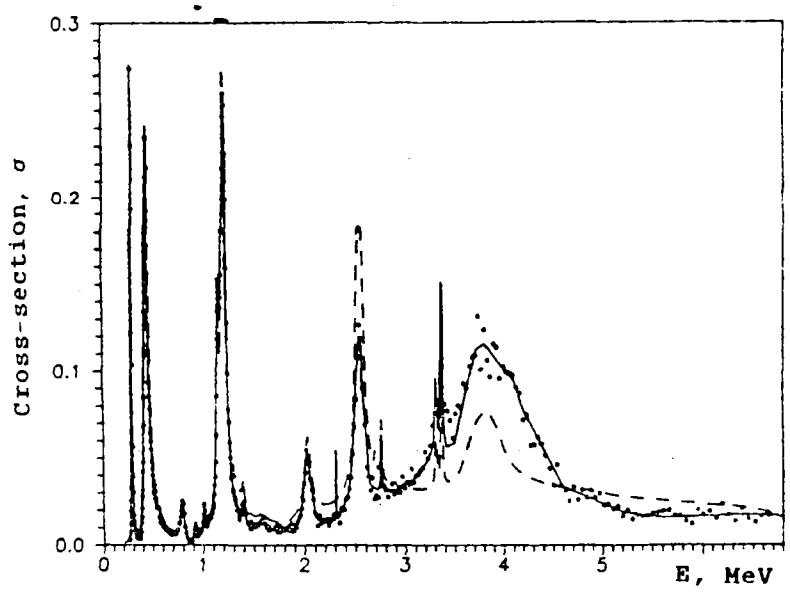

Fig.2. Same caption as for Fig. 1., for the (n,p_0) reaction. Experimental data taken from reference [2].

computational procedure included in the computer program CMT-80. The values of the σ_{non} reaction cross-sections obtained as a result of these calculations are in good agreement with the few existing experimental data [15]. The elastic scattering cross-sections, obtained in the framework of the optical model and using the parameters given in reference [3], are also in good agreement with the results of direct measurements published in [17-20]. Let us now review each of these processes:

1. The $^{14}N(n,n')^{14}N$ Reaction. The calculation of the inelastic neutron scattering excitation functions for 39 individual energy levels of ^{14}N up to an energy of 12.23 MeV were performed. The levels above that energy were analyzed in the approximation of a continuous spectrum. The values of the excitation functions of the discrete levels were in good agreement with contemporary measurements [20].

2. The $^{14}N(n,p)^{14}C$ Reaction. The calculation of the (n,p) reaction cross-section included the contribution of 10 excited levels of ^{14}C with energies up to 10.433 MeV. The continuous spectrum approximation was used above this energy. In the energy range of 10^{-5} eV to 0.43 MeV the values for the (n,p_0) process were taken from ENDF/B-IV [3]. The results of direct measurements [1] were used between 0.42 MeV and 7.0 MeV; these were either simply averaged or were approximated by linear interpolation on the basis of the evaluated data published in reference [3]. The results of statistical calculations were used above 7.0 MeV. Fig. 2 shows a comparison of the calculated $^{14}N(n,p_0)$ cross-section with ENDF/B-IV and experimental data [1].

3. The $^{14}N(n,d)^{13}C$ Reaction. The calculation of this cross-section was performed using the excitation functions for 18 discrete levels of the ^{13}C nucleus up to 11.72 MeV. The continuous spectrum approximation was used above 11.80 MeV.

4. The $^{14}N(n,t)^{12}C$ Reaction. The calculation of this cross-section was performed using the excitation functions for 9 discrete levels of the ^{12}C nucleus up to 12.71 MeV. The continuous spectrum approximation was used above 12.80 MeV.

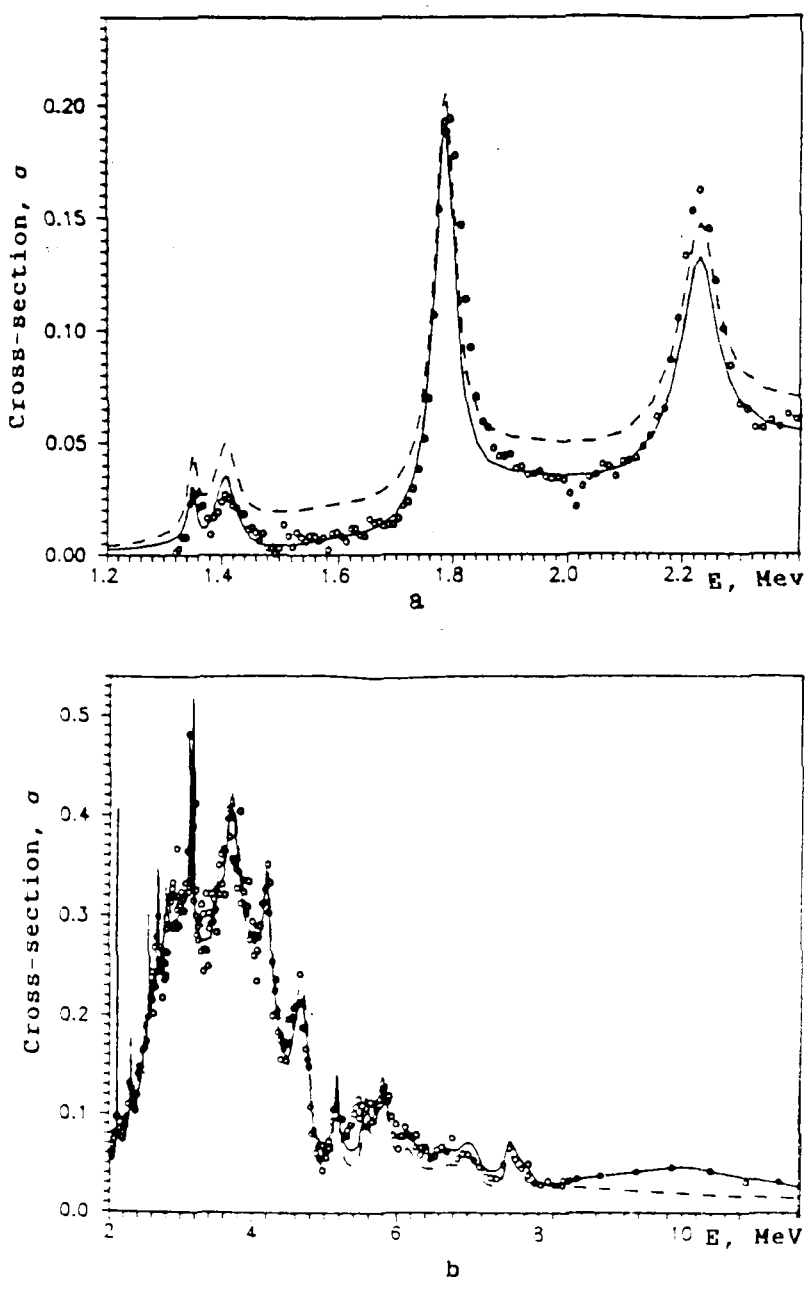

Fig. 3. Same caption as for Fig. 1, for the (n,α_0) reaction. Experimental data are taken from reference [1].

5. The $^{14}N(n,\alpha)^{11}B$ Reaction. The calculation of this reaction process included the contribution of 18 discrete excited levels of the ^{11}B nucleus with energies up to 10.96 MeV. The continuous spectrum approximation was used above 11.0 MeV. For the ground (E_0=0, I=3/2$^-$) and first excited (E_1=2.124 MeV, I=1/2$^-$) levels of the ^{11}B nucleus we used the averaged values of experimental results given in reference [1] in the energy ranges of 1.33 to 15.0 MeV and 4.0 to 14.5 MeV, respectively. Beyond these upper values we used results of statistical calculations, as we had done for all of the other levels from threshold to 20 MeV. A

DISCRETE LEVEL PARAMETERS FOR THE ^{14}N, ^{14}C, ^{13}C, ^{12}C AND ^{11}B NUCLIDES

Level No.	^{14}N		^{14}C		^{13}C		^{12}C		^{11}B	
	E,MeV	I^π	E,MeV	I^π	E,MeV	I^π	E,MeV	I^π	E,MeV	I^π
ground	0,0	1^+	0,0	0^+	0,0	$1/2^-$	0,0	0^+	0,0	$3/2^-$
1	2,312	0^+	6,093	1^-	3,086	$1/2^+$	4,439	2^+	2,124	$1/2^-$
2	3,944	1^+	6,589	0^-	3,684	$3/2^-$	7,655	0^+	4,445	$5/2^-$
3	4,913	0^-	6,728	3^-	3,854	$5/2^+$	9,641	3^-	5,020	$3/2^-$
4	5,105	2^-	6,901	0^-	3,864	$5/2^+$	10,30	0^+	6,742	$7/2^+$
5	5,691	1^-	7,011	2^+	7,492	$1/2^-$	10,844	1^-	6,792	$1/2^+$
6	5,833	3^-	7,341	2^-	7,549	$5/2^-$	11,160	2^+	7,285	$5/2^+$
7	6,197	1^+	8,318	2^+	7,677	$3/2^+$	11,828	2^-	7,978	$3/2^+$
8	6,443	3^+	9,801	1^+	8,350	$3/2^+$	12,710	1^+	8,559	$1/2^-$
9	7,028	2^-	10,433	2^+	8,858	$1/2^-$			8,920	$5/2^-$
10	7,966	2^-			9,499	$3/2^-$			9,186	$7/2^+$
11	8,061	1^-			9,899	$3/2^+$			9,275	$5/2^+$
12	8,489	4^+			10,460	$1/2^-$			9,870	$3/2^-$
13	8,617	0^-			10,753	$7/2^-$			10,260	$3/2^-$
14	8,800	0^-			10,809	$1/2^+$			10,330	$5/2^+$
15	8,907	3^-			11,000	$1/2^+$			10,450	$1/2^+$
16	8,963	5^+			11,078	$1/2^-$			10,601	$7/2^+$
17	8,978	3^+			11,721	$3/2^-$			10,960	$5/2^-$
18	9,129	2^+								
19	9,172	2^-								
20	9,388	2^-								
21	9,508	2^+								
22	9,702	1^+								
23	10,063	1^+								
24	10,228	1^-								
25	10,434	2^+								
26	10,560	1^-								
27	10,809	4^+								
28	11,040	1^+								
29	11,051	0^+								
30	11,100	2^+								
31	11,246	3^-								
32	11,300	2^-								
33	11,374	1^+								
34	11,516	3^+								
35	11,660	2^-								
36	11,750	1^+								
37	11,810	2^+								
38	11,950	2^-								
39	12,230	3^-								

comparison of the energy dependences of the (n,α_0) and (n,α_1) cross-sections with data given in references [1] and [3] are shown in Figs. 3a, 3b and 4.

6. The (n,np), (n,nα) and (n,2n) Reactions. These processes were analyzed in the framework of the evaporation model using the

level density parameters for the reaction product nuclides obtained from the description of the total strength function in the energy range of the neutron binding energy. Experimental data on the neutron resonance densities were taken from the compilation given in reference [11].

The angular distributions for all of the gamma rays associated with the above mentioned processes were assumed to be isotropic. The angular distributions for all of the charged particles and neutrons emitted in the (n,np), (n,nα) and (n,2n) threshold reactions were assumed to be isotropic in the centre of mass.

The neutron angular distributions for the inelastic scattering processes with excitation of discrete levels were calculated using the CMT-80 [12] computer program; these were then converted to laboratory coordinates in the form of Legendre coefficients. Experimental results reported in reference [20] were used for a number of discrete levels.

The neutron angular distributions for inelastic scattering were also calculated in the framework of the optical model in the energy ranges of $E_n = 10^{-5}$ eV to 7.70 MeV and for E_n > 14.0 MeV. Experimental data given in reference [20] were used in the energy interval of 7.70 to 14.0 MeV.

The energy spectra of the secondary neutrons in the (n,np), (n,nα), (n,2n), and (n,n') reactions were calculated in the continuum using the evaporation model. The principal parameter in this model is the thermal temperature of the residual nucleus as a function of the incident neutron energy. The energy dependence of the temperature T for the (n,n') process was represented by the following equation:

$$aT^2 = U = E_n - 2T \qquad (2)$$

where a is the level density parameter for ^{14}N,
2T is the average energy of the secondary neutron,
E_n is the initial neutron energy.

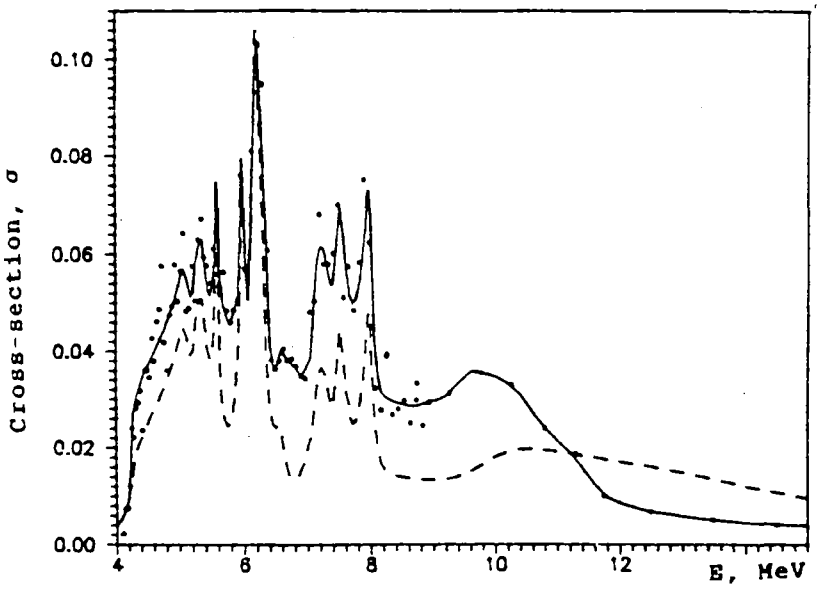

Fig. 4. Same caption as for Fig. 1, for the (n,α_1) reaction. Experimental data are taken from reference [1].

The level density parameters a of the residual nuclei were derived from the resolved resonance parameters given in reference [11]. For instance, for the ^{14}N target nucleus, using the simple Fermi gas model and data from reference [11], we obtained the value a = 1.437 MeV^{-1} . The dependence $T(E_n)$ for the (n,np), (n,nα) and (n,2n) processes was calculated using equation (2).

Normalized gamma ray transition probabilities were evaluated for all reactions with discrete level excitation in the residual nuclei. The basic data used for the evaluation of these quantities were taken from the compilations given in references [13] and [14].

The evaluation of the nuclear data for the ^{14}N isotope performed in this work has been compiled as a separate data file in ENDF/B-V format. This ^{14}N file has been incorporated (as MAT=710) in the working version of the BROND-1 data library, and can be obtained from the Nuclear Data Centre of the State Committee on Atomic Energy.

REFERENCES

[1] MORGAN, G.L., Nucl. Sci. and Eng. 70 (1979) 163.

[2] HEATON, S.H., et al., Bull. Am. Phys. Soc. 15 (1970) 568.

[3] YOUNG, P.G., FOSTER, D.G., Rep. LA-4725, Los Alamos National Laboratory (1972).

[4] CARLSON, A.D., et al., Nucl. Sci. and Eng. 42 (1970) 28.

[5] FOSTER, D., et al., Phys.Rev. 3C (1971) 576.

[6] BILPUCH, E.G., Rep. WASH-1034 , US Atomic Energy Commission, Washington D.C. (1961).

[7] BOMMER, J., Rep. HMI-B-210 (1976).

[8] BADIKOV, S.A., et al., Fixed ordinate method for the processing and analysis of experimental data, Preprint FEI-1328, Obninsk (1982) (in Russian).

[9] VINOGRADOV, V.N., et al., Analytical approximation of data in nuclear and neutron physics, Ehnergoatomizdat, Moscow (1987) (in Russian).

[10] BADIKOV, S.A., BLOKHIN, A.I., BULEEVA, N.N., et al., Problems of Atomic Science and Technology. Ser. Nuclear Constants 2 (1989) 39 (in Russian).

[11] MUGHABHAB, S.F., et al., Neutron cross-sections, Vol.1, Part A, Academic Press, New York (1981).

[12] TITARENKO, N.N., Program CMT-80. Calculation of binary reaction cross-sections in the framework of the statistical model, Preprint FEI-1260, Obninsk (1982) (in Russian).

[13] AJZENBERG-SELOVE, F., Nucl. Phys. A449 (1986) 1.

[14] LEDERER, C.M., SHIRLEY, V.S. (Eds.), Table of Isotopes, 7th Edn., Wiley-Interscience, New York (1978).

[15] DEKTAREV, Yu.Eh., et al., Atomnaya Ehnergiya 19 (1965) 456 (in Russian) and NYSTROEM, G., et al., Phys. Scripta 5 (1972) 175 (in Russian).

[16] PEREY, C.M., PEREY, F.G., At. and Nucl. Data Tables 13 (1974) 293.

[17] BABA, M., et al., in Proc. Conf. on Nuclear Data and Applications, Santa-Fe, N.M., 1 (1985) 223.

[18] PEREY, F.G., et al., Rep. ORNL-4805 , Oak Ridge National Laboratory (1974).

[19] TEMPLON, J.A., et al., Nucl. Sci. and Eng. 91 (1985) 451.

[20] CHARDINE, J., Rep. CEA-N-1506 (1986).

NEUTRON SPECTRA FROM (p,n) REACTIONS ON THE ^{165}Ho, ^{204}Pb, ^{206}Pb, ^{207}Pb, ^{208}Pb AND ^{209}Bi NUCLIDES AND THEIR NUCLEAR LEVEL DENSITIES

B.V. Zhuravlev, N.S. Biryukov, A.P. Rudenko,
N.N. Titarenko, V.I. Trykova

Abstract

Neutron spectra from the (p,n) reaction on the ^{165}Ho, ^{207}Pb, ^{208}Pb, and ^{209}Bi nuclei have been measured at a proton energy of 6.95±0.15 MeV. These experimental data, together with data obtained earlier at E_p=11 MeV on the ^{165}Ho, ^{204}Pb, ^{206}Pb, ^{207}Pb, ^{208}Pb and ^{209}Bi nuclei have been analyzed in the framework of the statistical nuclear reaction theory using the generalized model of a superfluid nucleus for the nuclear level density. The absolute nuclear level density has been determined for a wide range of excitation energies.

Introduction

In 1986, the International Atomic Energy Agency initiated a Coordinated Research Programme on the "Measurement and Analysis of Double Differential Neutron Emission Spectra in (p,n) and (α,n) Reactions" with the aim to obtain information on nuclear level densities. As part of this programme the Institute of Physics and Power Engineering (FEI) has been conducting measurements of the (p,n) reaction on deformed and near-magic nuclei.

In reports presented to the IAEA, we described the measurement and analysis of neutron spectra from (p,n) reactions on the ^{165}Ho, ^{181}Ta, ^{197}Au, ^{204}Pb, ^{206}Pb, ^{207}Pb, ^{208}Pb and ^{209}Bi nuclei at a proton energy of 11 MeV, which had been performed as part of IAEA research contracts 4322/R0/CF and 4322/R1/CF. This work continued in the form of additional measurements of neutron spectra from the ^{165}Ho, ^{207}Pb, ^{208}Pb and ^{209}Bi nuclei at a proton energy of 6.95±0.15 MeV, and their subsequent analysis in the framework of the statistical theory. The combined analysis of the data from these two sets of measurements at two different proton energies made it possible to determine the absolute nuclear level density in a wide excitation energy range.

Experiment

The measurements were made with a time-of-flight neutron spectrometer on the 150 cm FEI cyclotron [1]. The two proton energies were obtained by accelerating molecular hydrogen in an accelerating voltage frequency of 8.9 MHz. The targets consisted of foils having a thickness of 13.66, 18.90, 21.87, and 13.20 mg/cm^2 for ^{165}Ho (99.9%), ^{207}Pb (93.2%), ^{208}Pb (98.3%) and ^{209}Bi (99.8%), respectively. The average beam current at the target was 1 μA. The neutrons were detected by a scintillation counter with a stilbene crystal (70mm ϕ, 50mm h) and a FEhU-30 photomultiplier with the independent detection of neutrons and gamma rays [2]. The detector efficiency was determined by measuring the prompt ^{252}Cf neutron fission spectrum using the time-of-flight method with the simultaneous detection of the fission fragments using a fast ionization chamber [3]. The spectrum recommended by the US National Bureau of Standards was used as the standard [4]. The resolving power of the spectrometer, defined by the half-width of the gamma-ray peak, was 1.4 ns/m for a flight distance of 2.5 m. The channel width of the flight time analyzer was 0.89 ns. The minimum spectral neutron energy was 0.65 MeV.

The procedure for the measurement of the neutron spectrum consisted of measuring the current recorded by the integrating circuit, with a Faraday cup serving as current collector, both with and without target under the same proton beam conditions. The recorded ^{165}Ho spectrum is shown in Fig. 1. The background was negligible and was practically time uncorrelated. The ^{165}Ho and ^{209}Bi spectra were measured at angles ranging from 75° to 150° at 15° intervals. As can be seen in Fig. 2, the ^{165}Ho spectra measured at different angles fall within the limits of the measurement errors. It is to be expected that the angular distribution of reactions with a high Q_{pn} value, have an isotropic character. Consequently, the ^{207}Pb and ^{208}Pb spectra were measured only at an angle of 105°. The following factors were considered in the determination of the error of the measured neutron emission cross-sections:

1. The statistical measurement error varied from 1.5% at E_n=1 MeV to 20% for the maximum energies.

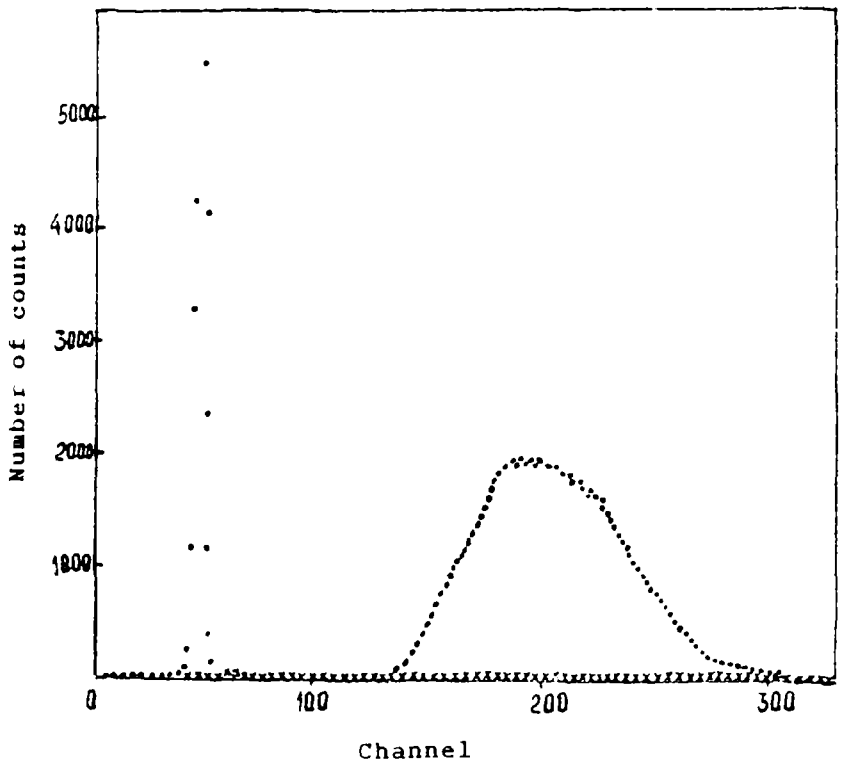

Fig. 1. Measured spectrum for the ^{165}Ho(p,n) reaction at an angle of θ=105°: • - signal plus background, x - background.

2. The error in the determination of the absolute efficiency of the neutron detector varied between 3% and 5%.

3. The uncertainty in the measurement of the proton beam current at the target was 3%.

4. The error in the determination of the atomic density in the target was 2%.

5. The error related to the calibration of the spectrometer was less than 2%.

The integral neutron spectra are given in Figs. 3-7.

Calculations

The analysis of the measured spectra was performed with the aid of the Hauser-Feshbach formalism and with nuclear level densities described according to the superfluid model of the nucleus taking surface effects and the contribution of collective states into consideration [5,6].

$$\rho(U,J) = \rho_{BCS}(U,J) \cdot K_{vib}(U) \cdot K_{rot}(U) \qquad (1)$$

$$K_{rot} = \begin{cases} 1 & \text{- for spherical nuclei} \\ F_{\perp} \cdot t & \text{- for deformed nuclei} \end{cases} \qquad (2)$$

$$K_{vib} = \exp\left\{ \sum_{J} (2\lambda_i + 1) \cdot \Lambda - \sum_{I} (2\lambda_i + 1) \cdot w_i \cdot \bar{n} / t \right\} \qquad (3)$$

where

$$\Lambda = (1+\bar{n}_i) \cdot \ln (1+\bar{n}_i) - (\bar{n}_i \cdot \ln \bar{n}_i)$$

and $F_{\perp}$ is the perpendicular moment of inertia,
w_i is the vibrational state energy,
λ_i is the degree of degradation,
$\bar{n}_i$ is the degree of population of vibrational excited states for a given temperature t.

$$\bar{n}_i = \frac{\exp\left[- \frac{C_V \cdot (w_i^2 + 4\pi^2 t^2)}{w_i} \right]}{\exp(-w_i / t) - 1} \qquad (4)$$

where C_V is a constant defining the enhancement of the vibrational component of the level density.

In the superfluid nucleus model, the nuclear level density can be represented by the following expression

$$\rho_{BCS} = \frac{(2J+1)}{2\sqrt{2\pi} \cdot \sigma_{eff}^3 \cdot Det^{1/2}} \cdot \exp\{S - \Phi\} \qquad (5)$$

where

$$\Phi = \frac{\left(J + \frac{1}{2}\right)^2}{2\sigma_{eff}^2}$$

The relationship between the entropy S, the term Det and other thermodynamic functions as well as the excitation energy is determined by equation (5) which describes the states of the superfluid nucleus.

The main parameters of this model are the correlation function Δ_0 and the level density parameter a. Above the critical point the

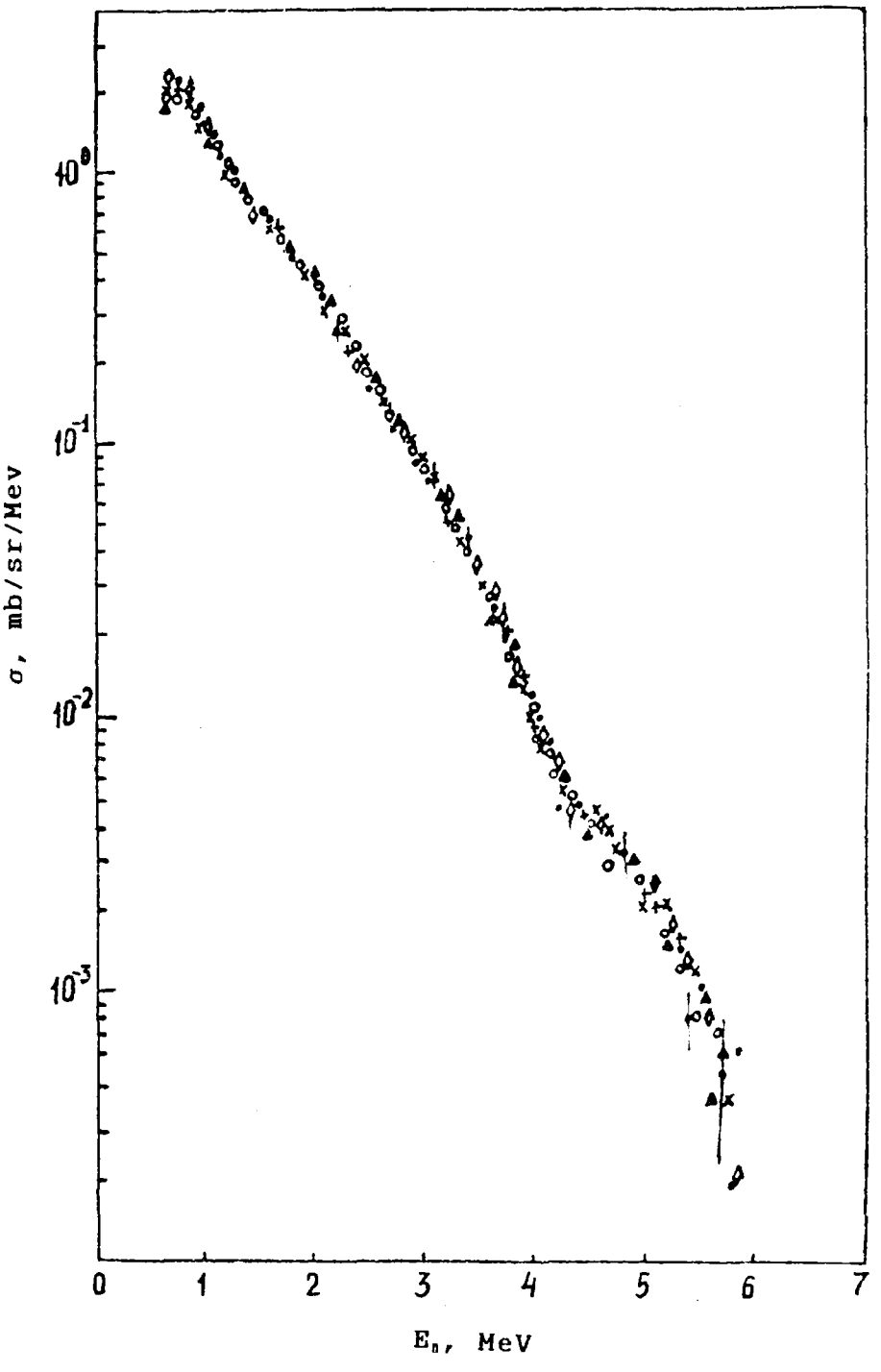

Fig. 2. ^{165}Ho(p,n) reaction neutron spectrum for E_p=6.95 MeV:

• - 75°, × - 90°, o - 105°,
▲ - 120°, + - 135°, ◊ - 150°

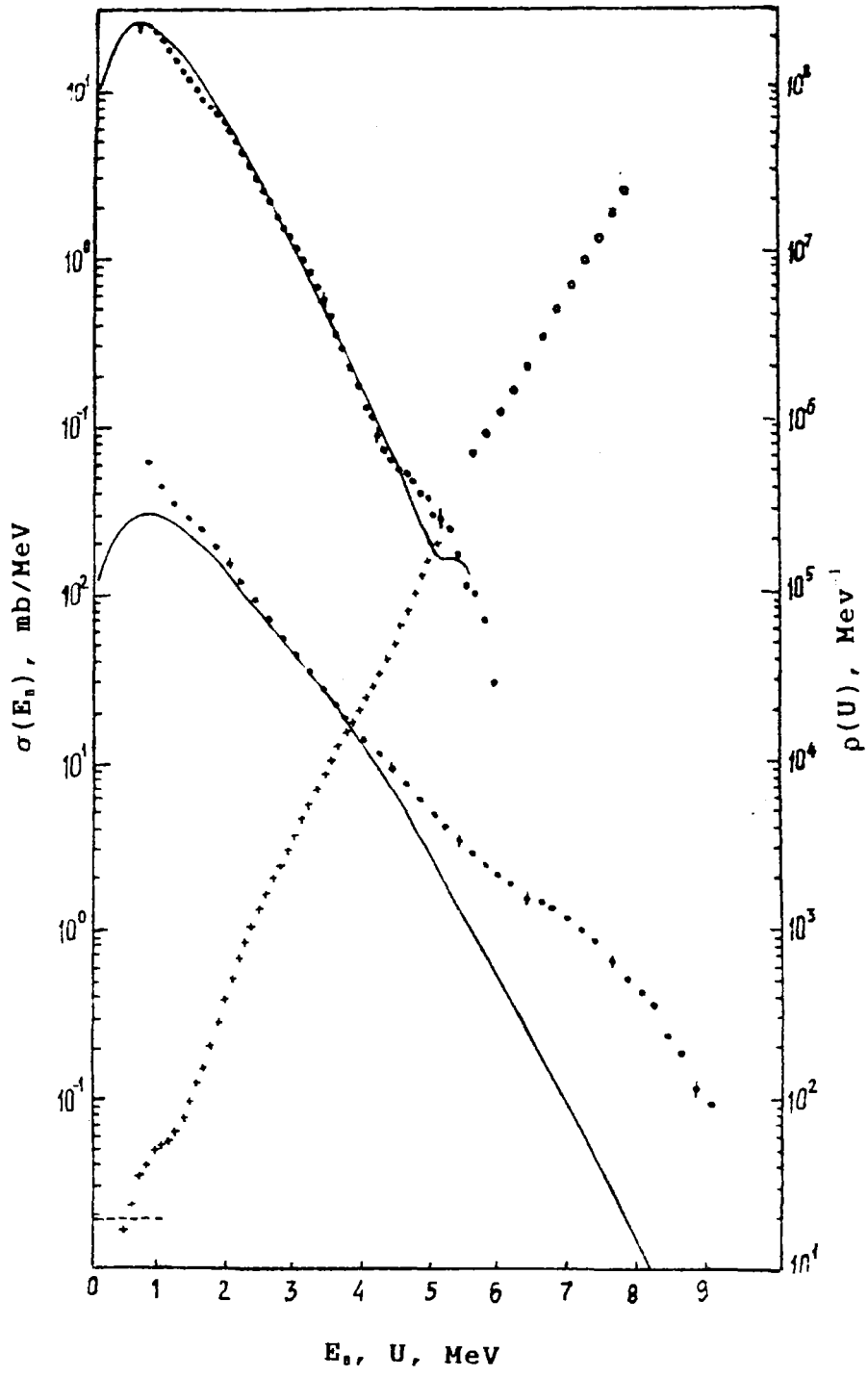

Fig. 3. $^{165}Ho(p,n)^{165}Er$ reaction integral neutron spectra for E_p=6.95 MeV (top curve) and E_p=11.2 Mev (bottom curve). Continuous curve - calculation. + and • - absolute level density (right-hand scale), determined from data for E_p=6.95 MeV and E_p=11.2 MeV, respectively. The horizontal dotted line shows the level density at low excitation energies according to the level scheme given in reference [16].

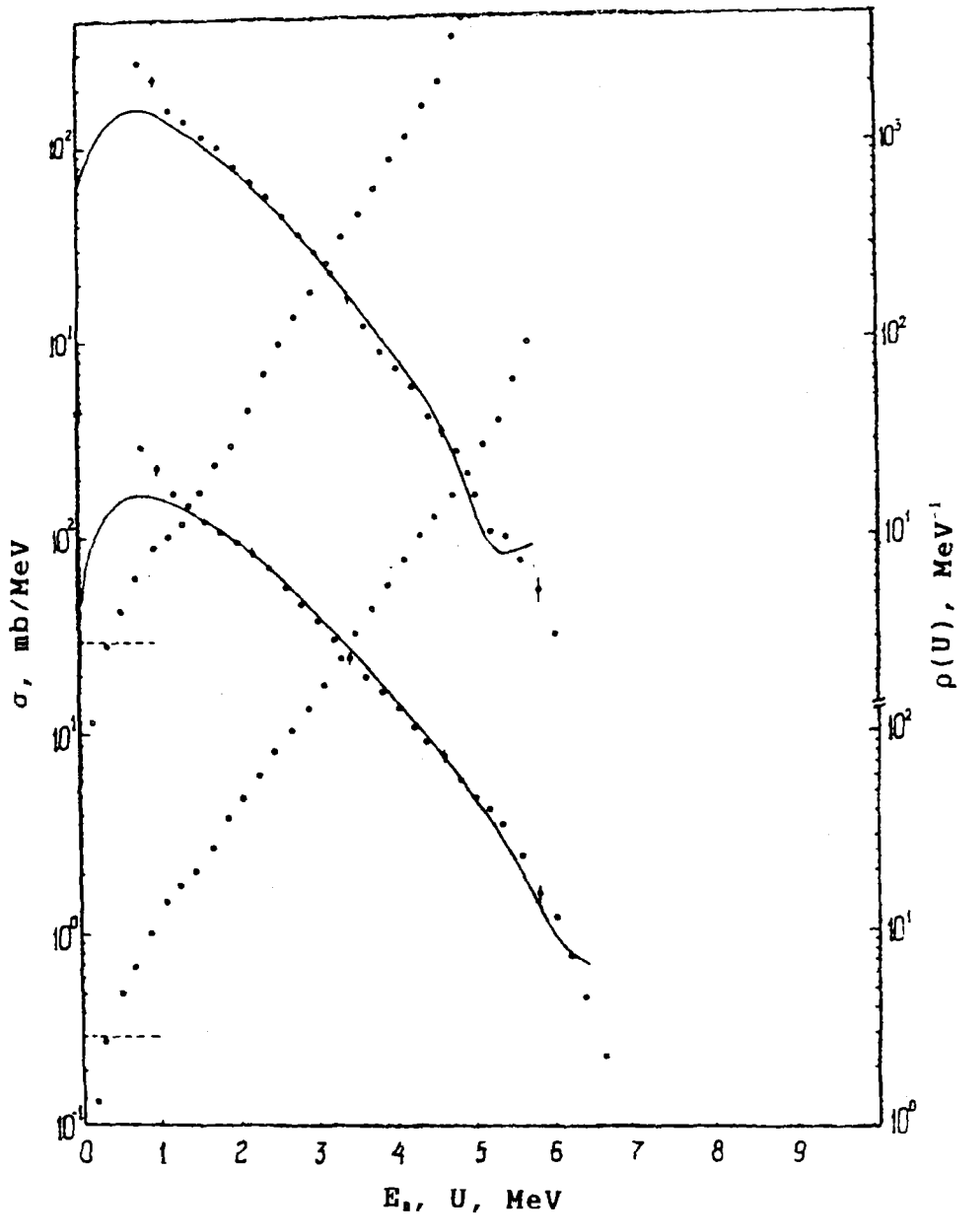

Fig. 4 Integral neutron spectra for the $^{204}Pb(p,n)^{204}Bi$ reaction (top curve) and for the $^{206}Pb(p,n)^{206}Bi$ reaction (bottom curve). Same nomenclature as in Fig. 3.

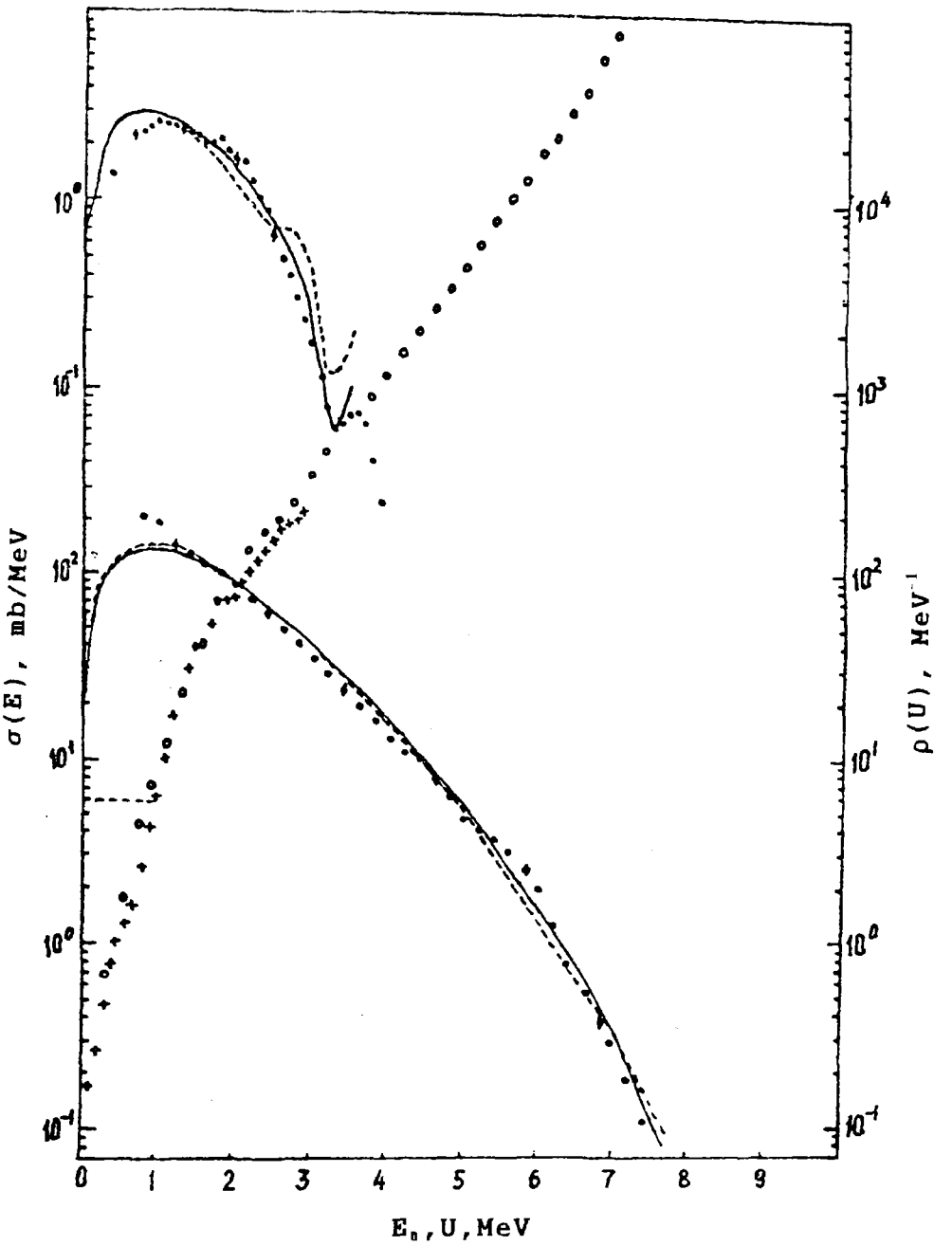

Fig. 5 $^{207}Pb(p,n)^{207}Bi$ reaction integral neutron spectra for E_p=6.95 MeV (top curve) and for 11.2 MeV (bottom curve). Dashed line - superfluid nucleus model calculation; Continuous line - Fermi-gas model calculation with reverse shift (a=12.5 MeV and Δ=-0.9 MeV)

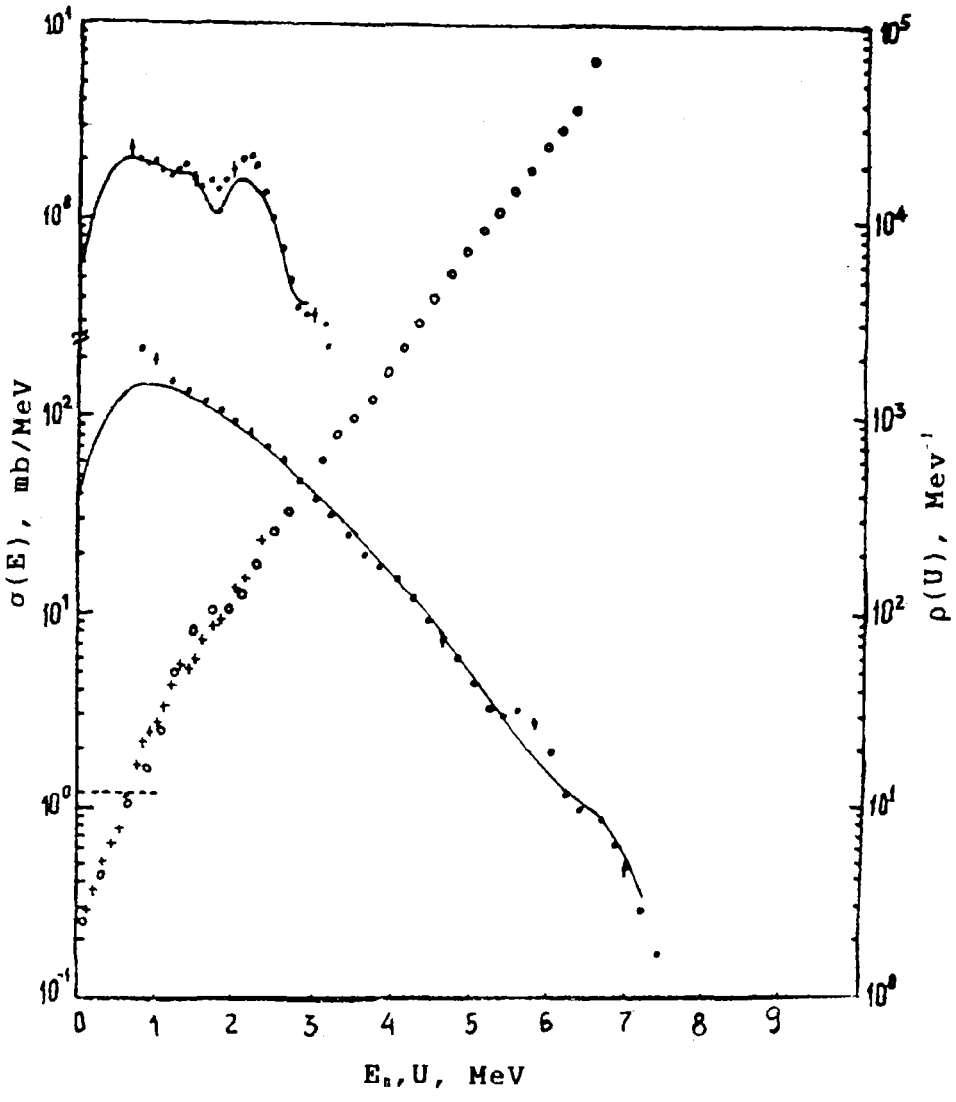

Fig. 6 $^{208}Pb(p,n)^{208}Bi$ reaction integral neutron spectra for E_p=6.95 MeV (top curve) and for E_p=11.2 MeV (bottom curve). Same nomenclature as in Fig.3.

superfluid nucleus model equations differ from the Fermi-gas model in that the excitation energy is replaced by the condensation energy $E_{cond}=(3/2\pi^2)\cdot a_{cr}\cdot\Delta_0^2)$.

In order to take the shell effects into account, the authors of reference [5] suggested using the empirical dependence of the a parameter on the excitation energy and the shell corrections in the nuclear binding energy $\delta W(Z,A)$.

$$a(U,Z,A)=\begin{cases}\tilde{a}\cdot A & for\ U>U_{cr}\\ a_{cr}(U_{cr},Z,A) & for\ U\le U_{cr}\end{cases} \qquad (6)$$

where

$$A = \left[1 + (1 - \exp (\gamma \cdot U_{eff})) \cdot \frac{\delta W(Z,A)}{U_{eff}} \right]$$

Differences in the thermodynamic functions for even-odd nuclei were effectuated by shifting the ground state energy.

$$U = U_{eff} + \begin{Bmatrix} 0 \ for\ even\text{-}even\ nuclei \\ \Delta_o \ for\ odd\ nuclei \\ 2\Delta_o \ for\ odd\text{-}odd\ nuclei \end{Bmatrix} \qquad (7)$$

The correlation function for a single component description was determined by the energy increments Δ_{0Z} and Δ_{0N} [7] in the following manner:

$$\Delta_0 = \frac{\sqrt{\Delta^2_{ON} + \Delta^2_{OZ} \cdot (Z/N)^{1/3}}}{\sqrt{1 + (Z/N)^{1/3}}} \qquad (8)$$

All of the calculations in the framework of the optical-statistical model were performed with the use of the SMT-80 computer code. For excitation energies smaller than the value of U_c transitions were calculated to discrete levels. In order to compare the cross-sections with experimental data they were averaged over the excitation energy in accordance with normal procedures. The spread in the distribution corresponded to the energy resolution of the spectrometer. Particle emission spectra above the U_c energy were calculated by subdividing the whole excitation energy range into equal energy intervals of ≈0.2 MeV. Each interval was assumed to have up to 30 different spin states of a given parity, and the same number for another parity, with a probability $\rho(U,J)$. These quasi-levels were processed with the computer program as discrete nuclear states having effective transmission coefficients. Calculations were performed using the global optical potential systematics described in references [9] and [10].

Equations 1 through 8 show that the generalized superfluid nucleus model relies on a number of parameters, namely a, Δ_0, δW, γ, C_v and w_i . Some of these can be derived from experimental

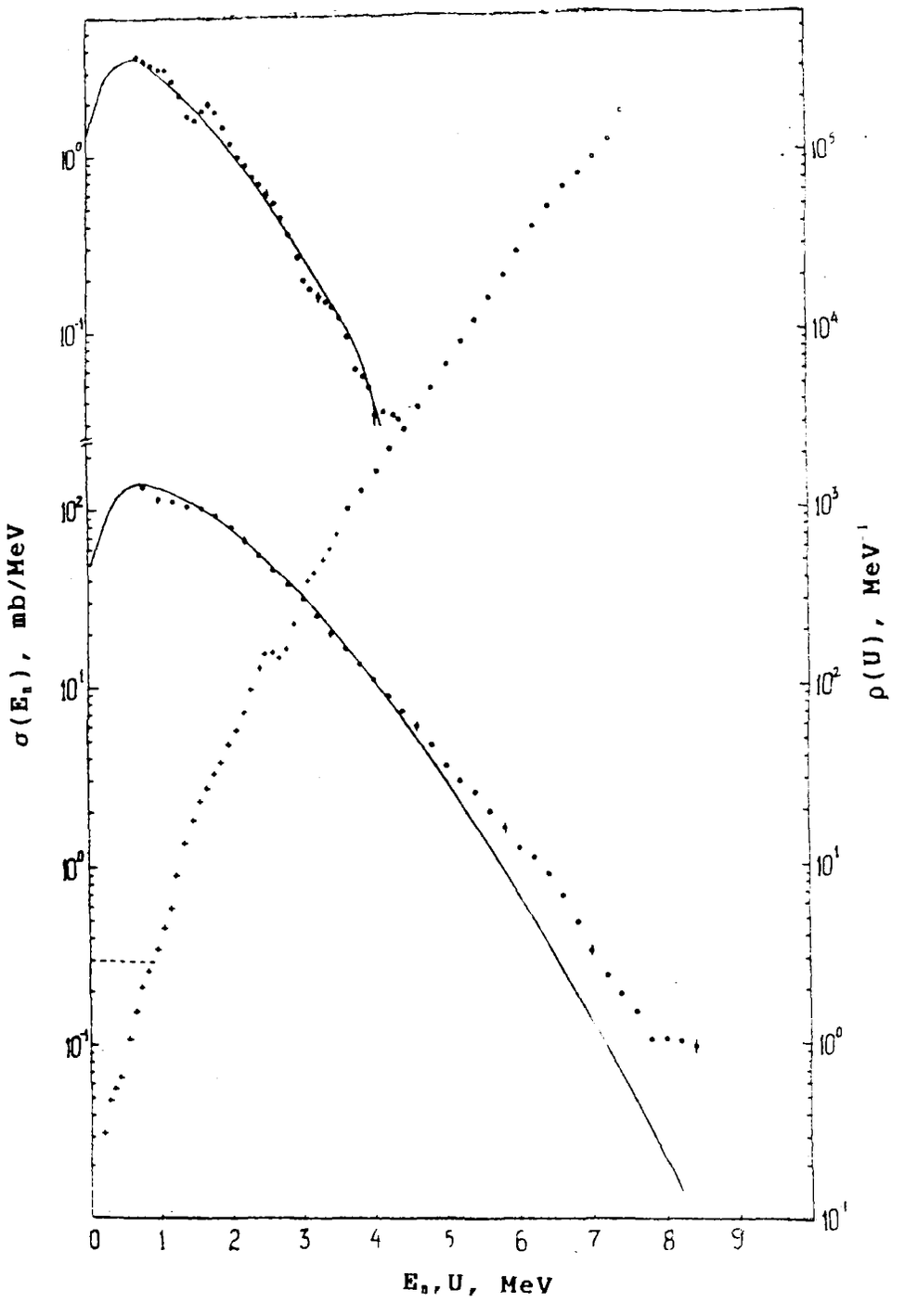

Fig. 7. $^{209}Bi(p,n)^{209}Po$ reaction integral neutron spectra for E_p=6.95 MeV (top curve) and E_p=11.2 MeV (bottom curve). Same nomenclature as in Fig. 3.

data. In the investigations described in references [5] and [6], values for the quantity ă were obtained from the analysis of the experimentally determined $\rho(B_n,J)$ data, yielding the dependence

$$ă=0.0931\cdot A$$

The correlation functions for the proton Δ_{0Z} and neutron Δ_{0N} systems, determined on the basis of measurements of nuclear mass differences reported in reference [7], were used to calculate the quantity Δ_0 by means of equation (8).

Values of shell corrections δW were determined in reference [11] on the basis of experimental data on the mass-defect value and its liquid drop model component. The value for the γ parameter, which reflects the energy dependence of the nuclear level density parameter, is recommended to be 0.064 MeV^{-} in reference [5], and $0.4/A^{1/3}$ MeV^{-} in reference [12]. Both of these recommended values were obtained from an analysis of neutron resonance density data $\rho(B_n,J)$ which is restricted to a relatively narrow excitation energy range, and which holds true for an A-averaged dependence. Inasmuch as the energy values of the first vibrational states w_1 and the values of the enhancement coefficients for odd and odd-odd nuclei, investigated in this work, differed significantly from recommendations based on even-even nuclei, the values of the γ, w_1 and C_γ) parameters used in these calculations were adjusted so as to agree with measured neutron spectra.

Results

The neutron spectra resulting from (p,n) reactions on the ^{165}Ho, ^{204}Pb, ^{206}Pb, ^{207}Pb, ^{208}Pb and ^{209}Bi nuclides, which have been measured in this experiment at proton energies of 6.95 and 11.2 MeV, are shown in Figs. 2 to 7; the results of the calculations and the model parameters are listed in the Table below. Initially, the calculations were made for $E_p=6.95\pm0.15$ MeV since the contribution from non-equilibrium processes can be omitted at this energy. The internal consistency of the absolute values of the cross-sections was achieved by varying the proton energy within the limits of its uncertainty. A satisfactory description

of the (p,n) reaction spectra was observed for the ^{165}Ho, ^{208}Pb and ^{209}Bi nuclides. A somewhat better agreement between theory and experiment was achieved for ^{207}Pb using the Fermi-gas model with the parameter values a=12.5 MeV^{-1} and Δ=-0.9 MeV. The neutron spectra at E_p=11.2 MeV were then calculated with parameters determined at the proton energy of 6.95 MeV. The comparison of the calculated and measured spectra for ^{207}Pb and ^{208}Pb indicates that the (p,n) reaction mechanism for these nuclides at E_p=11.2 MeV are compound in their nature. This observation gives grounds to assume that the same mechanism applies to the ^{204}Pb and ^{206}Pb nuclides whose reactions have larger threshold energy $Q_{p,n}$, and to be able to derive nuclear level density parameters from the measured spectra. As the value of $Q_{p,n}$ decreases, which corresponds to an increase in the energy of the emitted neutrons as well as in the nuclear excitation energy, neutron emission appears to become unbalanced in the upper end of the spectrum in reactions involving ^{209}Bi, and to a larger extent in reactions involving ^{165}Ho.

Let us discuss the values of those nuclear level density parameters which can be adjusted or varied so as to arrrive at an optimum description of the measured neutron spectra. The γ parameter for the ^{165}Er, ^{204} Bi and ^{206}Bi nuclides agrees very well with the recommendations given in reference [12], but it is approximately 1.5 times smaller for the ^{207}Bi, ^{208}Bi and ^{209}Pb nuclides, this points to a weaker energy dependence of the nuclear level density parameter a for nuclides close to the double magic number nuclides 82 and 126. The enhancement of the vibrational component of the level densities, calculated with equations (3) and (4), is strongly dependent on the energies of the first 2+ states for which there is a vast amount of experimental data for even-even spherical nuclei. The w_{2+} values which were calculated for the ^{204}Bi and ^{209}Po nuclides are close to the known values of 0.96 MeV and 0.66 MeV for ^{202}Pb and ^{208}Po, respectively; for the ^{206}Bi, ^{207}Bi and ^{208}Bi nuclides, however, these values are two times smaller than the corresponding values for ^{204}Pb and ^{206}Pb. The values for the vibrational enhancement coefficients C_γ are close to those recommended in reference [6] (namely $C_\gamma=0.005\cdot A^{1/3}$ MeV^{-1}), which were derived from an analysis of observed widths of giant quadrupole isoscalar resonances.

If the values of measured neutron emission cross-sections, including the excitation of known low-lying levels, can be reproduced by calculations, then it is possible to derive the values of the absolute nuclear level densities from a comparison of calculated and measured spectra in a wide range of excitation energies [15]:

$$\rho(U) = \rho(U)_{model} \frac{(\delta\sigma / \delta E_n)_{meas}}{(\delta\sigma / \delta E_n)_{calc}} \qquad (10)$$

Values for the absolute nuclear level densities for the ^{165}Er, ^{204}Bi, ^{206}Bi, ^{207}Bi, ^{208}Bi and ^{209}Po nuclides as a function of excitation energy, calculated according to equation (10), are given in Figs. 3 to 7. At low excitation energies, there is good agreement with the level counting data for all nuclides, and for Er there is also agreement with the data on the average distances between neutron resonances $\bar{D}_0$ (see Table). The error in the determination of the absolute nuclear level density according to equation (10) can be estimated from the accuracy achieved in measuring the $(\delta\sigma/\delta E_n)/\sigma_{level}$ (which was ≈ 10-15%), which was determined by the uncertainties in the neutron optical potential (≈ 10%) and the spin dependence (≈ 7%). On this basis, we estimate the accuracy of the absolute level density to be ≈ 15 to 20%.

Conclusions

Neutron spectra from the (p,n) reactions on the ^{165}Ho, ^{207}Pb, ^{208}Pb and ^{209}Bi nuclides were measured for proton energies of 6.95±0.15 MeV. The experimental data from this experiment combined with earlier data measured at an energy of E_p=11 MeV have been analyzed in the framework of the Hauser-Feshbach formalism using the generalized superfluid nucleus model for the level densities. The determined level density parameters correspond to the optimal description of the neutron spectra measured in the range of discrete states as well as in the continuum. The following observation were made: a weakening of the energy dependence of the a parameter for nuclides in the vicinity of the double magic

nuclei 82 and 126, and a decrease in the energy of the first vibrational state W_{2+} for ^{206}Bi, ^{207}Bi and ^{208}Bi in comparison with the even-even ^{204}Pb and ^{206}Pb nuclides. The absolute nuclear level density was determined for a wide range of excitation energies by comparing the model calculations with the measured neutron spectra. The results agree with the data on level counting at low excitation energies, and for ^{165}Er there is also good agreement with the data on the average distances between neutron resonances.

PARAMETERS FOR THE GENERALIZED SUPERFLUID MODEL OF THE NUCLEUS

Parameter	^{165}Er	^{204}Bi	^{206}Bi	^{207}Bi	^{208}Bi	^{209}Po
O.P.	p [9] n [10]	p [9] n [9]	p [9] n [9]	p [9] n [9]	p [9] n [9]	p [9] n[10]
U_C , MeV	0.92	1.00	1.00	1.00	1.00	1.00
N_{level}	20	3	3	6	12	3
$\tilde{a}$, MeV^{-1}	15.40	19.00	19.18	19.27	19.36	19.46
Δ_0 , MeV	1.04	0.70	0.58	0.54	0.47	0.62
δW, MeV	-0.17	-8.65	-9.42	-9.96	-11.09	-9.71
γ , MeV	0.073	0.070	0.070	0.050	0.047	0.048
K_{rot}	$\mathcal{J}_\perp \cdot t$ (β=0.3)	1	1	1	1	1
C_V , MeV^{-1}	0.0300	0.0294	0.0295	0.0296	0.0296	0.0250
W_{2+} , MeV	0.50	0.90	0.45	0.30	0.35	0.50
W_{3-} , MeV	1.00	1.44	1.43	1.43	1.42	1.42
$\bar{D}_0$, eV	23 20±3 [13] 22 [14]	383	753	109	313	1925
$Q_{p,n}$, MeV	-1.155	-5.177	-4.433	-3.188	-3.651	-2.675

REFERENCES

[1] BARYBA, V,Ya., BIRYUKOV, N.S., ZHURAVLEV, B.V., et al., Neutron Spectra and Angular Distributions from (p,n) Reactions, Preprint FEI-910, Institute of Physics and Power Engineering, Obninsk (1979) (in Russian).

[2] BIRYUKOV, N.S., ZHURAVLEV, B.V., Experimental Instruments and Techniques 6 (1983) 22 (in Russian).

[3] BARYBA, V.Ya., KORNILOV, N.V., et al., Problems of Atomic Science and Technology, Ser. Reactor Engineering 5(19) (1977) 45 (in Russian).

[4] GRUNDL, J., EISEHAUER, C., in Neutron Standards and Applications (Proc. Int. Symp., Gaithersburg MD, 1977), US National Bureau of Standards Special Publication 493, US Government Printing Office, Washington, DC (1977).

[5] IGNATYUK, A.V., ISTEKOV, K.K., SMIRENKIN, G.N., Yadernaya Fizika 29 4 (1979) 875 (in Russian).

[6] GRUDZEVICH, O.T., IGNATYUK, A.B., PLYASKIN, V.I., in Proc. First Int. Conf. on Neutron Physics, Kiev, 1987. Nauka, Moscow, Vol. 2 (1988) 96 (in Russian).

[7] SOLOVIEV, V,G., Theory of Complex Nuclei, Nauka, Moscow (1971) (in Russian).

[8] TITARENKO, N.N., Computer Program SMT-80. Calculation of Cross-sections of Binary Reactions in the Framework of the Statistical Model, Preprint FEI-1260, Institute of Physics and Power Engineering, Obninsk (1982) (in Russian).

[9] BECHETTI, F.D., GREENLESS, G.W., Phys. Rev. 182 (1969) 1190.

[10] HOLMQUIST, B., WIEDLING, T., J. Nucl. Energy 27 (1973) 543.

[11] MEYERS, W.D., SWIATECKI, W.S., Ark. Fys. 36 (1967) 593.

[12] RAMAMURTHY, V.S., et al., in Basic and Applied Problems of Nuclear Level Densities (Proc. IAEA Advisory Group Meeting, Brookaven, 1983) (BHAT, M.R., Ed.), Brookhaven National Lab., Upton, NY, Rep. BNL-NCS-51694 (1983).

[13] MUGHABGHAB, S.F., Neutron Cross-Sections, Vol.1 Part B (1984).

[14] DILG, W., et al.,Nucl. Phys. A217 (1973) 269.

[15] VONACH, H., in Basic and Applied Problems of Nuclear Level Densities (Proc. IAEA Advisory Group Meeting, Brookhaven, 1983) (BHAT, M.R., Ed.), Brookhaven National Lab., Upton, NY, Rep. BNL-NCS-51694 (1983). (1983).

[16] BROWNE, E., et al., Table of Isotopes, 7th ed. (LEDERER, C.M., SHIRLEY, V.S. Eds), Wiley, New York (1978).